lariat leading to intron excision and ligation of the upstream and downstream exons (Query et al., 1996).

In addition to the "classical" spliceosomal mechanisms, splicing is modulated by exonic/intronic splicing enhancers/silencers (ESE, ISE, ESS, ISS). The *trans*-factors for the splicing enhancers/silencers carry repeats of arginine and serine are accordingly called SR proteins. Tissue-specific and developmental stage-specific expressions of the splicing *trans*-factors enable precise spatial and temporal regulations of the gene expressions. In addition, the splicing *trans*-factors also work on constitutively spliced exons to compensate for highly degenerative "classical" splicing *cis*-elements.

3 Disorders Associated with Disruption of Splicing *Cis*-Elements

3.1 Aberrations of the 5′ Splice Sites

Mutations disrupting the 5′ splice sites have been most frequently reported. U1 snRNA recognizes three nucleotides at the end of an exon and six nucleotides at the beginning of an intron (Fig. 2). The completely matched nucleotides to U1 snRNA are CAG|GTAAGT, where the vertical line represents the exon/intron boundary. The completely matched sequence is observed at 1597 sites out of the entire 189,249 5′ splice sites in the human genome (Sahashi et al., 2007), which is the tenth most common sequence. The completely matched 5′ splice site is rather avoided because, in the second stage of splicing, U1 snRNA is substituted for U5 snRNA. If U1 snRNA is tightly bound to the 5′ splice site, it hinders binding of U5 snRNA.

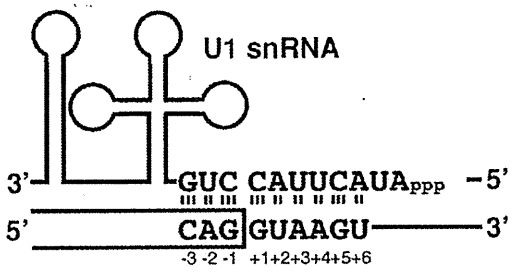

Fig. 2 U1 snRNA recognizes three nucleotides at the 3′ end of an exon and six nucleotides at the 5′end of an intron

Degeneracy of the 5′ splice site and its vulnerability to disease-causing mutations have been extensively studied. Three algorithms have been proposed. First, Shapiro and Senapathy collated nucleotide frequencies at each position of the 5′ splice site. They assumed that nucleotide frequencies at each position of the 5′ splice site represent the splicing signal intensity. They thus constructed a linear regression model so that the most preferred 5′ splice site becomes 1.0 and the most unfavorable 5′ splice site becomes 0.0 (Shapiro and Senapathy, 1987). Second, Rogan and Schneider

invented the information contents, R*i*. For example, at a specific position, if a single nucleotide is exclusively used, the information content at this position becomes– $\log_2(1/4) = 2$ bits. Similarly, if two nucleotides are equally used, the information content becomes $-\log_2(2/4) = 1$ bit. In R*i*, the similarity to the consensus sequence is represented by the sum of information bits (Rogan and Schneider, 1995; O'Neill et al., 1998). Third, we found that a new parameter, the SD-Score, which represents a common logarithm of the frequency of a specific 5′ splice site in the human genome, efficiently predicts the splicing signal intensity (Sahashi et al., 2007).

Our algorithm predicts the splicing consequences of mutations with the sensitivity of 97.1% and the specificity of 94.7%. Simulation of all the possible mutations in the human genome using the SD-score algorithm predicts high frequencies of splicing mutations from exon –3 to intron +6 (Table 1). Especially at exon position –3, about one third of mutations are predicted to cause aberrant splicing. Using our algorithm, we predicted and proved that *DYSF* G1842D in Miyoshi myopathy, *ABCD1* R545W in adrenoleucodystrophy, *GLA* Q333X in Fabry disease, and *DMD* Q119X and Q1144X in Duchenne muscular dystrophy are not missense or nonsense mutations but are splicing mutations. Algorithms by us and by others all point to the notion that aberrant splicing caused by mutations at the 5′ splice sites is likely to be underestimated.

Table 1 Predicted ratios of exonic and intronic splicing mutations

Position	–3	–2	–1	+1	+2	+3	+4	+5	+6
Complementary nucleotide	C (%)	A (%)	G (%)	G	T	A (%)	A (%)	G (%)	T (%)
A	1.8	–	93.7	–	–	–	–	93.9	56.9
C	–	89.6	99.7	–	–	99.9	94.4	98.6	75.4
G	35.0	90.5	–	–	–	48.7	96.2	–	56.7
T	76.7	86.2	97.1	–	–	99.9	94.3	97.0	–
All mutations	37.8	88.8	96.8	–	–	82.8	95.0	96.5	63.0

3.2 Human Branch Point Consensus Sequence

In an effort to seek an algorithm to predict the position of the branch point sequence (BPS) in humans, we sequenced 367 clones of lariat RT-PCR products arising from 52 introns of 20 human housekeeping genes and identified that the human consensus BPS is simply yUnAy, where "y" represents U or C (Gao et al., 2008) (Fig. 3). The consensus BPS was more degenerative than we had expected and we failed to construct a dependable algorithm that predicts the position of the BPS. Sixteen disease-causing mutations and a polymorphism, however, have been reported to date that disrupt a BPS and cause aberrant splicing (Gao et al., 2008). Among these, eight mutates U at position –2, whereas nine affects A at position 0, which also supports the notion that U at –2 and A at 0 are essential nucleotides.

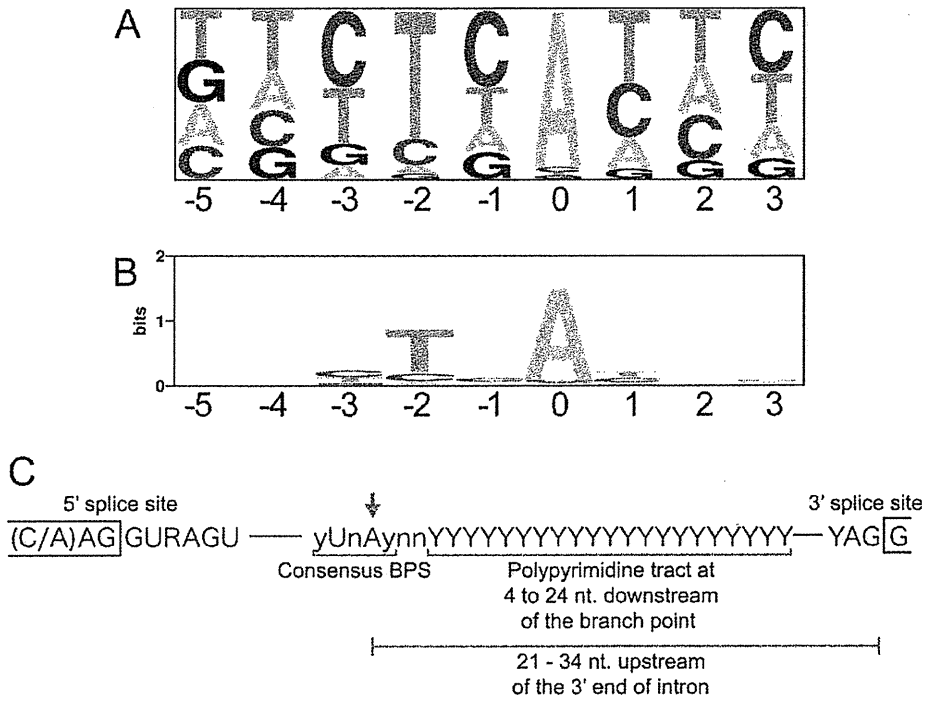

Fig. 3 Human consensus BPS. (**a**) Pictogram and (**b**) WebLogo presentations of BPS. Position 0 represents the branch point. (**c**) Representative sequences and positions of splicing *cis*-elements

3.3 Ectopic AG Dinucleotide Abrogates the AG-Scanning Mechanism

The 3′ end of an intron and the 5′ end of an exon carry a consensus sequence of CAG|G, where the vertical line represents the intron/exon boundary. The AG dinucleotide is scanned from the branch point and the first AG is recognized as the 3′ end of the intron (Chen et al., 2000). In a patient with congenital myasthenic syndrome, we identified duplication of a 16-nt segment comprised of 8 intronic and 8 exonic nucleotides at the intron 10/exon 10 boundary of *CHRNE* encoding the acetylcholine receptor epsilon subunit (Ohno et al., 2005). We found that the upstream AG of the duplicated segment is exclusively used for splicing and that one or two mutations in the upstream BPS had no effect whereas complete deletion of the upstream BPS partially activated the downstream AG. Similar exclusive activation of the upstream AG is reported in *HEXB* (Dlott et al., 1990) and *SLC4A1* (Bianchi et al., 1997). Creation of a cryptic AG dinucleotide close to the 3′ end of an intron should be carefully scrutinized in mutation analysis.

3.4 Mutations That Disrupt ESE *and* ESS

Gorlov and colleagues predicted that more than 16–20% of missense mutations are splicing mutations that disrupt an ESE (Gorlov et al., 2003). According to our own

experience, their estimates are likely to be too high. Most ESE/ESS-disrupting mutations, however, are likely to be underestimated, because the positions and sequences of ESE/ESS are highly degenerative.

Four Web services provide valuable information to locate ESE and ESS. First, the ESE Finder (http://rulai.cshl.org/ESE/) calculates the similarity of a given nucleotide sequence to the consensus sequences of four splicing *trans*-factors, SF2/ASF, SC35, SRp40, and SRp55 (Cartegni et al., 2003; Smith et al., 2006). Second, the RESCUE-ESE Web server (http://genes.mit.edu/burgelab/rescue-ese/) shows the similarity of a given sequence to ESE elements of unidentified splicing *trans*-factors (Fairbrother et al., 2002). The same group also provides the FAS-ESS Web service to screen for ESS elements (http://genes.mit.edu/fas-ess/) (Wang et al., 2004). Third, the PESX Web server (http://cubweb.biology.columbia.edu/pesx/) indicates an RNA octamer with putative exonic splicing enhancing or silencing activities (Zhang and Chasin, 2004; Zhang et al., 2005). Fourth, the ESRsearch Web server (http://ast.bioinfo.tau.ac.il/) shows 285 candidate ESE/ESS sequences (Goren et al., 2006), as well as ESE/ESS elements indicated by the RESCUE-ESE, FAS-ESS, and PESX services.

In patients with congenital myasthenic syndromes, we identified that *CHRNE* E154X and EF157V (Ohno et al., 2003), as well as *COLQ* E415G (Kimbell et al., 2004), disrupt an ESE and cause aberrant splicing. The ESE/ESS servers above indicate disruption of candidate splicing *cis*-elements for all three mutations, but we frequently obtain false positives and we cannot simply rely on the servers. Analysis of patient mRNA or analysis using a minigene is generally expected.

3.5 Mutations That Disrupt ISE *and* ISS

Identification of mutations disrupting intronic splicing *cis*-elements is more challenging than that of exonic mutations, because introns are longer than exons and splicing mutations can be anywhere in the introns, and because we do not have a dependable algorithm to predict ISE/ISS. The ESRsearch Web server described above is able to indicate consensus sequences recognized by a variety of splicing *trans*-factors including intronic ones.

In a patient with congenital myasthenic syndrome, we identified that *CHRNA1* IVS3-8G>A attenuates binding of *hnRNP H* ~100-fold and causes exclusive inclusion of the downstream exon P3A (Masuda et al., 2008) (Fig. 4). We also identified that polypyrimidine tract binding protein (PTB) silences recognition of exon P3A and tannic acid facilitates the expression of PTB by activating its promoter region (Gao et al., 2009).

3.6 Spinal Muscular Atrophy (SMA)

SMA is an autosomal recessive disorder characterized by degeneration of the anterior horn cells of the spinal cord, which causes muscular weakness and atrophy. SMA is caused by loss-of-function mutations including deletion of the *SMN1* gene

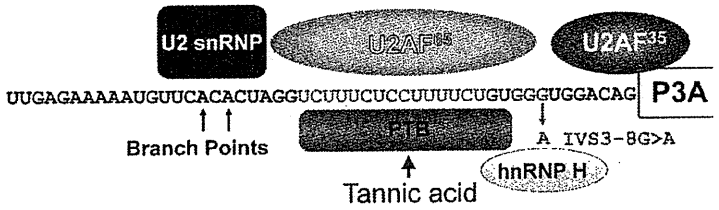

Fig. 4 *CHRNA1* carries a 75-nt exon P3A. Its inclusion generates a nonfunctional alpha subunit of the acetylcholine receptor. hnRNP H and PTB silence recognition of exon P3A and induce its skipping. The IVS3-8G>A mutation identified in a patient with congenital myasthenic syndrome weakens the binding of hnRNP H and causes inclusion of exon P3A. Tannic acid facilitates the expression of PTB and partially ameliorates aberrant splicing due to IVS3-8G>A

that encodes the survival of motor neuron 1. Humans carry almost identical *SMN1* and *SMN2* genes both on chromosome 5q13. *SMN2* carries a C-to-T transition at position 6 of exon 7 compared to *SMN1*, which results in loss of an SF2/ASF-dependent ESE activity (Cartegni et al., 2006). In addition, *SMN2* carries an A-to-G transition at position +100 of intron 7, which creates a high-affinity hnRNP A1-binding site and promotes skipping of exon 7 (Kashima et al., 2007). Skipping of exon 7 in *SMN2* can be ameliorated by therapeutic doses of valproic acid (Brichta et al., 2003, 2006) and of salbutamol (Angelozzi et al., 2008).

4 Skipping of Multiple Exons Caused by a Single Splicing Mutation

4.1 Skipping of Multiple Contiguous Exons

A mutation disrupting a splicing *cis*-element generally affects splicing of a single exon or intron, but sometimes generates aberrant transcripts affecting multiple neighboring exons. Skipping of multiple contiguous exons is accounted for by ordered removal of introns and consequent clustering of neighboring exons (Schwarze et al., 1999; Takahara et al., 2002).

4.2 Nonsense-Associated Skipping of a Remote Exon (NASRE)

A single mutation infrequently causes skipping of a remote exon. In a patient with congenital myasthenic syndrome, we found that a 7-nt deletion in exon 7 of *CHRNE* causes complete skipping of the preceding exon 6. *CHRNE* exon 6 is composed of 101 nucleotides. It carries weak splicing signals and is partially skipped even in normal subjects. The exon 6-skipped transcript, however, is removed by the nonsense-mediated mRNA decay (NMD) mechanism. The 7-nt deletion in exon 7 restores the open reading frame of the exon 6-skipped transcript and renders it immune to NMD. On the other hand, the normally spliced transcript carries a

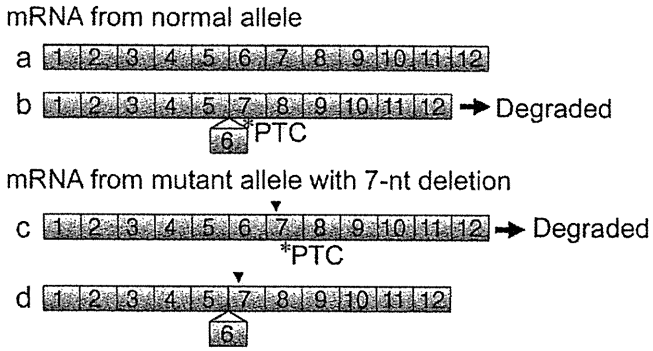

Fig. 5 NASRE. Wild-type *CHRNE* generates the normally spliced transcript (**a**) and the exon 6-skipped transcript (**b**), because exon 6 carries weak splicing signals. The exon-skipped transcript carries a premature termination codon (PTC) and is degraded by NMD. A 7-nt deletion (*arrowhead*) in exon 7 generates a PTC in the normally spliced transcript (**c**) and is degraded by NMD. The deletion resumes the open reading frame from the exon 6-skipped transcript, and the transcript escapes NMD (**d**)

premature stop codon (PTC) after the 7-nt deletion, and is degraded by NMD[1] (Fig. 5). We dubbed this mechanism NASRE, and found that it is in effect in *SLC25A20* (Hsu et al., 2001), *DBT* (Fisher et al., 1993), *BTK* (Haire et al., 1997), and *MLH1* (Clarke et al., 2000).

5 Disorders Associated with Dysregulation of Splicing *Trans*-Factors

5.1 Myotonic Dystrophy

Myotonic dystrophy is an autosomal dominant multisystem disorder affecting skeletal muscles, eye, heart, endocrine system, and central nervous system. The clinical symptoms include variable degrees of muscle weakness and wasting, myotonia, cataract, insulin resistance, hypogonadism, cardiac conduction defects, frontal balding, and intellectual disabilities (Harper and Monckton, 2004). Myotonic dystrophy is caused by abnormally expanded CTG repeats in the 3′ untranslated region of the *DMPK* gene encoding the dystrophia myotonica protein kinase on chromosome 19q13 (myotonic dystrophy type 1, DM1) (Brook et al., 1992) or by abnormally expanded CCTG repeats in intron 1 of the *ZNF9* gene encoding the zinc finger protein 9 on chromosome 3q21 (myotonic dystrophy type 2, DM2) (Liquori et al., 2001). In DM1, normal individuals have 5–30 repeats, mildly affected patients

[1]Nonsense-mediated mRNA decay (NMD). NMD is a quality-assurance mechanism that degrades mRNAs harboring a premature termination codon (PTC) (Chang et al., 2007). Proteins translated from mRNAs harboring PTCs potentially have dominant-negative or deleterious activities. In pre-mRNA splicing, an exon–junction complex (EJC) is deposited 20–24 nucleotides upstream of each exon–exon junction. Ribosomes remove EJCs, but, in the presence of a PTC, EJCs stay on the transcript and trigger the NMD pathway in the cytoplasm.

have 50–80 repeats, and severely affected individuals have 2000 or more copies of CTG (Gharehbaghi-Schnell et al., 1998). In DM2, the size of expanded repeats is extremely variable, ranging from 75 to 11,000 repeats, with a mean of 5000 CCTG repeats (Liquori et al., 2001).

In both DM1 and DM2, expanded CTG or CCTG repeats in the noncoding regions sequestrate a splicing *trans*-factor muscleblind encoded by *MBNL1* to intranuclear RNA foci harboring the mutant RNA, and somehow upregulate another splicing *trans*-factor CUG-binding protein encoded by *CUGBP1* (Ranum and Cooper, 2006) (Fig. 6). Dysregulation of the two splicing *trans*-factors then causes aberrant splicing of their target genes. The aberrantly spliced genes identified to date in skeletal and cardiac muscles include *ATP2A1* (*SERCA1*) exon 22, *ATP2A2* (*SERCA2*) intron 19, *CAPN3* exon 16, *CLCN1* intron 2 and exons 6b/7a, *DMD* exons 71 and 78, *DTNA* exons 11A and 12, *FHOD1* (*FHOS*) exon 11a, *GFPT1* (*GFAT1*) exon 10, *INSR* exon 11, *KCNAB1* exons 2b/2c, *LDB3* (*ZASP*) exon 11 (189-nt exon 7 according to RefSeq Build 36.3), *MBNL1* exon 7 (54-nt exon 6 according to RefSeq), *MBNL2* exon 7 (54 nt, no exonic annotation in RefSeq), *MTMR1* exons 2.1 and 2.2, *NRAP* exon 12, *PDLIM3* (*ALP*) exons 5a/5b, *RYR1* exon 70, *TNNT2* exon 5, *TNNT3* fetal exon, *TTN* exons Zr4 and Zr5 (138-nt exon 11 and 138-nt exon 12 according to RefSeq), and *TTN* exon Mex5 (303-nt exon 315 according to RefSeq) (Philips et al., 1998; Savkur et al., 2001; Kimura et al., 2005; Lin et al., 2006). Lin and colleagues report that alternative transcripts observed in myotonic dystrophy are all fetal isoforms (Lin et al., 2006). Muscleblind normally translocates

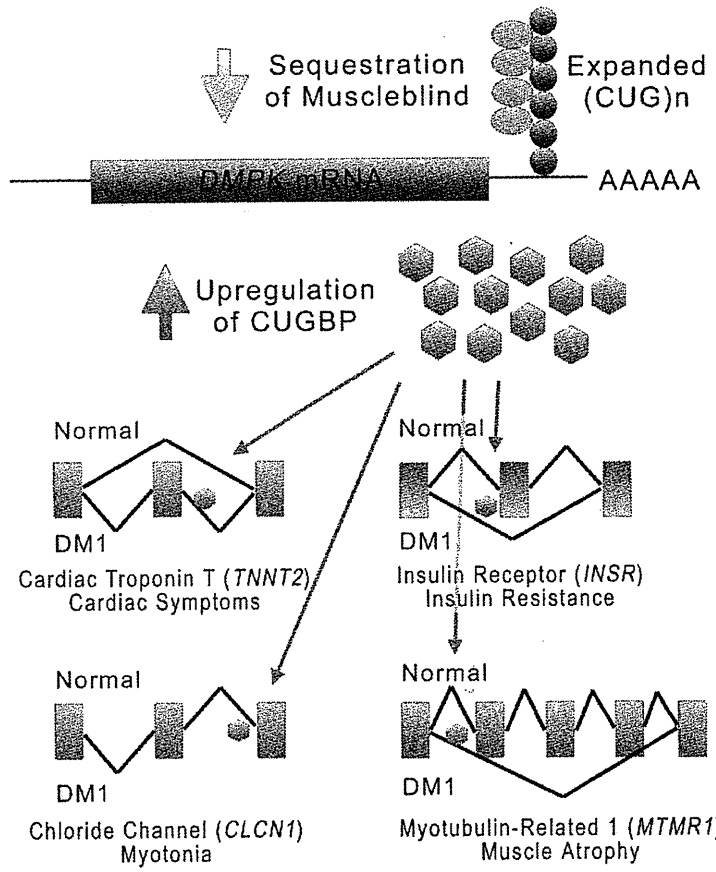

Fig. 6 In DM1, expanded CUG repeats in the 3′ UTR of DMPK sequestrate muscleblind and upregulates CUG-binding protein. Dysregulation of these splicing *trans*-factors causes aberrant splicing of their inherent target genes. Four representative target genes are indicated

from cytoplasm to nucleus in the postnatal period to induce adult-type splicings, and lack of muscleblind in nucleus due to sequestration to RNA foci recapitulates fetal splicing patterns.

5.2 *Alzheimer's Disease (AD) and Frontotemporal Dementia with Parkinsonism Linked to Chromosome 17 (FTDP-17)*

AD is the most common neurodegenerative disease representing dementia. It is characterized by intracellular neurofibrillary tangles (NFTs) and extracellular amyloid plaques. NFTs are composed of aggregates of the hyperphosphorylated tau protein encoded by *MAPT*. The amyloid plaques are composed of amyloid β peptide (Aβ) that originates from enzymatic cleavage of the amyloid precursor protein (*APP*) by β-secretase followed by γ-secretase (LaFerla et al., 2007). The γ-secretase is an enzyme complex composed of presenilin-1 (*PS1*) or presenilin-2 (*PS2*), as well as nicastrin, anterior pharynx defective (APH-1), and presenilin enhancer 2 (PEN-2) (Takasugi et al., 2003). Autosomal dominant forms of AD constitute ~5% of AD and are caused by mutations in *APP*, *PS1*, or *PS2* (Bertram and Tanzi, 2008).

Although the pathomechanisms underlying sporadic AD remain mostly unknown, *PS2* exon 5 is exclusively skipped in brains of sporadic AD, which is mediated by overexpression of a splicing *trans*-factor, *HMGA1a* (Sato et al., 1999; Manabe et al., 2003). As hypoxia induces the overexpression of HMGA1a, the upregulation of HMGA1a in sporadic AD may or may not represent an agonal state of AD, in which respiratory insufficiency possibly associated with pneumonia frequently becomes the cause of death.

Mutations in *MAPT* are not observed in AD, but are present in FTDP-17. *MAPT* exon 10 is alternatively spliced in normal brain. N279K, K280del, and L284L mutations on exon 10 provoke aberrant splicing of exon 10 by disrupting or enhancing exonic splicing *cis*-elements, and cause FTDP-17 (D'Souza et al., 1999) (Fig. 7). The splicing *trans*-factors for these *cis*-elements are also identified (Jiang et al., 2004; Kondo et al., 2004).

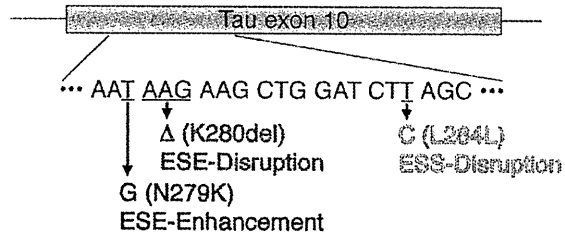

Fig. 7 Mutations on *MAPT* exon 10 cause excessive skipping (N279K and L284L) or inclusion (K280del) of exon 10

5.3 *Facioscapulohumeral Muscular Dystrophy (FSHD)*

FSHD is the third most common hereditary muscular dystrophy after Duchenne muscular dystrophy and myotonic dystrophy. As its name represents, the disease predominantly affects the face, the scapulae, and the proximal arm muscles. In

FSHD, the number of a 3.3 kb repeat in the subtelomeric region of 4q (4q35), designated *D4Z4*, are abnormally reduced (Wijmenga et al., 1992). Loss of *D4Z4* causes upregulation of FRG1 located upstream of *D4Z4* (Gabellini et al., 2002). FRG1 is a splicing *trans*-factor, and its overexpression causes aberrant splicing of *TNNT3* encoding the troponin T type 3 of fast skeletal muscle and *MTMR1* encoding the myotubularin-related protein 1 (Gabellini et al., 2006). The reported splicing aberrations in FSHD, however, have not been confirmed by us (unpublished data) or by the other groups (personal communications).

5.4 Fragile X-Associated Tremor/Ataxia Syndrome (FXTAS)

Fragile X mental retardation syndrome is caused by abnormal expansion of a CGG repeat in the 5′ untranslated region of *FMR1*, which culminates in hypermethylation of *FMR1* and silences its expression (Kremer et al., 1991). On the other hand, moderate expansion of the CGG repeat in *FMR1* causes FXTAS, which is characterized by intention tremor, Parkinsonism, cognitive decline, and neuropathy (Hagerman and Hagerman, 2004). In FXTAS, CGG-binding proteins including *hnRNP A2* and muscleblind are excessively bound to the expanded CGG repeats of *FMR1* and are depleted from the cellular pool (Iwahashi et al., 2006), which results in the loss their functions in other regulatory processes (Jacquemont et al., 2007).

5.5 Prader–Willi Syndrome (PWS)

PWS is an autosomal dominant disorder characterized by obesity, muscular hypotonia and weakness, mental retardation, short stature, hypogonadotropic hypogonadism, and small distal extremities. The proximal long arm of chromosome 15 (15q11-q13) is normally imprinted in order to achieve parent-specific monoallelic gene expressions. Some genes in this region are expressed only from the maternal allele, and some others are only from the paternal allele. Lack of a functional paternal copy of 15q11-13 causes PWS, whereas lack of a functional maternal copy of *UBE3A* in the same region results in *Angelman syndrome* (Horsthemke and Wagstaff, 2008). PWS is caused by a deletion of the paternal 15q11-q13 or by maternal uniparental disomy 15.

A *snoRNA HBII-52* is located in the defective region of PWS. HBII-52 binds to an ESS in exon Vb of *HTR2C* encoding the serotonin receptor 2C, and its disruption in PWS causes aberrant splicing of *HTR2C* and potentially accounts for dysfunctional serotonergic system in PWS (Kishore and Stamm, 2006).

5.6 Rett Syndrome

Rett syndrome is a neurodevelopmental disorder in females, which is characterized by loss of speech, stereotypical movements of hands, microcephaly, seizures, and

mental retardation. Rett syndrome is caused by a mutation in *MECP2* encoding the metyl-CpG-binding protein 2 (Amir et al., 1999). MeCP2 binds to a splicing *trans*-factor *YB-1* and the abnormal regulation of YB-1 causes aberrant splicing of its target genes (Young et al., 2005).

5.7 Spinocerebellar Ataxia Type 8 (SCA8)

SCA8 is caused by an abnormal expansion of CTA/CTG repeats in the protein-noncoding *ATXN8OS*, which represents the *ATXN8* opposite strand (Ikeda et al., 2008). Expanded CUG repeats on the *ATXN8OS* transcript potentially bind to and sequestrate CUG-binding proteins, as we observe in myotonic dystrophy (Mutsuddi and Rebay, 2005). In addition, *ATXN8* on the opposite strand of *ATXN8OS* encodes the Kelch-like 1, and the expanded CAG repeats on *ATXN8* give rise to a polyglutamine tract that forms a cytotoxic aggregate in neuronal cells (Moseley et al., 2006). Furthermore, expression of *ATXN8OS* is colocalized with that of *ATXN8* (Chen et al., 2008). *ATXN8OS* thus potentially serves as an antisense RNA for *ATXN8*, and the abnormal CTA/CTG expansion in *ATXN8OS* may dysregulate the expression of *ATXN8* (Fig. 8).

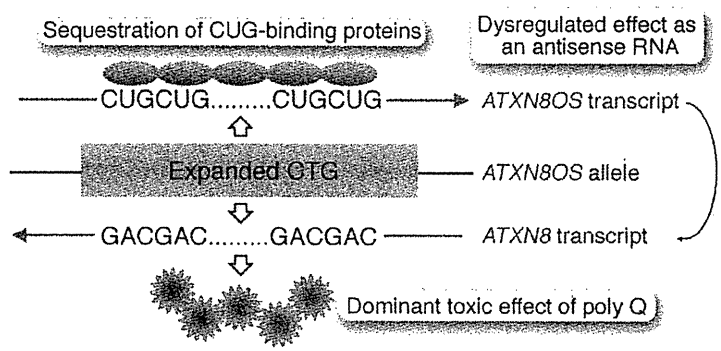

Fig. 8 Expanded CTG on *ATXN8OS* exerts three toxic effects on the bidirectional transcripts

5.8 Paraneoplastic Neurological Disorders (PND)

In PND, tumors outside of the nervous system excrete humoral factors such as hormones and cytokines, or provoke an immune response against specific molecules expressed in tumors, and cause a wide range of neurological symptoms. In paraneoplastic opsoclonus myoclonus ataxia (POMA), autoantibodies are raised against the Nova family of neuron-specific splicing *trans*-factor (Jensen et al., 2000; Ule et al., 2003, 2006; Licatalosi et al., 2008). In paraneoplastic encephalomyelitis and sensory neuropathy (PEN/SN or Hu syndrome), autoantibodies recognize the Hu family of RNA-binding protein (Szabo et al., 1991), a human homologue of the *Drosophila* splicing *trans*-factor *Elav* (Koushika et al., 2000; Soller and White, 2003). In both disorders, autoantibodies downregulate the splicing *trans*-factors and cause aberrant splicing in neuronal cells.

Acknowledgments Works from the authors' laboratories have been supported by Grants-in-Aid from the Ministry of Education, Culture, Sports, Science, and Technology of Japan, and from the Ministry of Health, Labor, and Welfare of Japan.

References

Abovich N, Rosbash M (1997) Cross-intron bridging interactions in the yeast commitment complex are conserved in mammals. Cell 89:403–412

Amir RE, Van den Veyver IB, Wan M, Tran CQ, Francke U et al (1999) Rett syndrome is caused by mutations in X-linked MECP2, encoding methyl-CpG-binding protein 2. Nat Genet 23: 185–188

Angelozzi C, Borgo F, Tiziano FD, Martella A, Neri G et al (2008) Salbutamol increases SMN mRNA and protein levels in spinal muscular atrophy cells. J Med Genet 45:29–31

Arning S, Gruter P, Bilbe G, Kramer A (1996) Mammalian splicing factor SF1 is encoded by variant cDNAs and binds to RNA. RNA 2:794–810

Bertram L, Tanzi RE (2008) Thirty years of Alzheimer's disease genetics: the implications of systematic meta-analyses. Nat Rev Neurosci 9:768–778

Bian Y, Masuda A, Matsuura T, Ito M, Okushin K et al (2009) Tannic acid facilitates expression of the polypyrimidine tract binding protein and alleviates deleterious inclusion of *CHRNA1* exon P3A due to an hnRNP H-disrupting mutation in congenital myasthenic syndrome. Hum Mol Genet 18:1229–1237

Bianchi P, Zanella A, Alloisio N, Barosi G, Bredi E et al (1997) A variant of the EPB3 gene of the anti-Lepore type in hereditary spherocytosis. Br J Haematol 98:283–288

Black DL (2003) Mechanisms of alternative pre-messenger RNA splicing. Annu Rev Biochem 72:291–336

Brichta L, Hofmann Y, Hahnen E, Siebzehnrubl FA, Raschke H et al (2003) Valproic acid increases the SMN2 protein level: a well-known drug as a potential therapy for spinal muscular atrophy. Hum Mol Genet 12:2481–2489

Brichta L, Holker I, Haug K, Klockgether T, Wirth B (2006) In vivo activation of SMN in spinal muscular atrophy carriers and patients treated with valproate. Ann Neurol 59:970–975

Brook JD, McCurrach ME, Harley HG, Buckler AJ, Church D et al (1992) Molecular basis of myotonic dystrophy: expansion of a trinucleotide (CTG) repeat at the 3′ end of a transcript encoding a protein kinase family member. Cell 68:799–808

Cartegni L, Hastings ML, Calarco JA, de Stanchina E, Krainer AR (2006) Determinants of exon 7 splicing in the spinal muscular atrophy genes, SMN1 and SMN2. Am J Hum Genet 78: 63–77

Cartegni L, Wang J, Zhu Z, Zhang MQ, Krainer AR (2003) ESEfinder: a web resource to identify exonic splicing enhancers. Nucleic Acids Res 31:3568–3571

Chang YF, Imam JS, Wilkinson MF (2007) The nonsense-mediated decay RNA surveillance pathway. Annu Rev Biochem 76:51–74

Chen S, Anderson K, Moore MJ (2000) Evidence for a linear search in bimolecular 3′ splice site AG selection. Proc Natl Acad Sci U S A 97:593–598

Chen WL, Lin JW, Huang HJ, Wang SM, Su MT et al (2008) SCA8 mRNA expression suggests an antisense regulation of KLHL1 and correlates to SCA8 pathology. Brain Res 1233: 176–184

Clarke LA, Veiga I, Isidro G, Jordan P, Ramos JS et al (2000) Pathological exon skipping in an HNPCC proband with MLH1 splice acceptor site mutation. Genes Chromosomes Cancer 29:367–370

Crick F (1970) Central dogma of molecular biology. Nature 227:561–563

Dlott B, d'Azzo A, Quon DV, Neufeld EF (1990) Two mutations produce intron insertion in mRNA and elongated beta-subunit of human beta-hexosaminidase. J Biol Chem 265: 17921–17927

D'Souza I, Poorkaj P, Hong M, Nochlin D, Lee VM et al (1999) Missense and silent tau gene mutations cause frontotemporal dementia with parkinsonism-chromosome 17 type, by affecting multiple alternative RNA splicing regulatory elements. Proc Natl Acad Sci U S A 96: 5598–5603

Fairbrother WG, Yeh RF, Sharp PA, Burge CB (2002) Predictive identification of exonic splicing enhancers in human genes. Science 297:1007–1013

Fisher CW, Fisher CR, Chuang JL, Lau KS, Chuang DT et al (1993) Occurrence of a 2-bp (AT) deletion allele and a nonsense (G-to-T) mutant allele at the E2 (DBT) locus of six patients with maple syrup urine disease: multiple-exon skipping as a secondary effect of the mutations. Am J Hum Genet 52:414–424

Gabellini D, D'Antona G, Moggio M, Prelle A, Zecca C et al (2006) Facioscapulohumeral muscular dystrophy in mice overexpressing FRG1. Nature 439:973–977

Gabellini D, Green MR, Tupler R (2002) Inappropriate gene activation in FSHD: a repressor complex binds a chromosomal repeat deleted in dystrophic muscle. Cell 110:339–348

Gao K, Masuda A, Matsuura T, Ohno K (2008) Human branch point consensus sequence is yUnAy. Nucleic Acids Res 36:2257–2267

Gharehbaghi-Schnell EB, Finsterer J, Korschineck I, Mamoli B, Binder BR (1998) Genotype-phenotype correlation in myotonic dystrophy. Clin Genet 53:20–26

Gilbert W (1986) Origin of life: the RNA world. Nature 319:618

Goren A, Ram O, Amit M, Keren H, Lev-Maor G et al (2006) Comparative analysis identifies exonic splicing regulatory sequences – The complex definition of enhancers and silencers. Mol Cell 22:769–781

Gorlov IP, Gorlova OY, Frazier ML, Amos CI (2003) Missense mutations in hMLH1 and hMSH2 are associated with exonic splicing enhancers. Am J Hum Genet 73:1157–1161

Hagerman PJ, Hagerman RJ (2004) The fragile-X premutation: a maturing perspective. Am J Hum Genet 74:805–816

Haire RN, Ohta Y, Strong SJ, Litman RT, Liu YY et al (1997) Unusual patterns of exon skipping in bruton tyrosine kinase are associated with mutations involving the intron 17 3′ splice site. Am J Hum Genet 60:798–807

Harper PS, Monckton DG (2004) Myotonic dystrophy. In: Engel AG (ed) Myology, 3rd edn. McGraw-Hill, New York, NY, pp 1039–1076

Horsthemke B, Wagstaff J (2008) Mechanisms of imprinting of the Prader–Willi/Angelman region. Am J Med Genet A 146A:2041–2052

Hsu BY, Iacobazzi V, Wang Z, Harvie H, Chalmers RA et al (2001) Aberrant mRNA splicing associated with coding region mutations in children with carnitine-acylcarnitine translocase deficiency. Mol Genet Metab 74:248–255

Ikeda Y, Daughters RS, Ranum LP (2008) Bidirectional expression of the SCA8 expansion mutation: one mutation, two genes. Cerebellum 7:150–158

Iwahashi CK, Yasui DH, An HJ, Greco CM, Tassone F et al (2006) Protein composition of the intranuclear inclusions of FXTAS. Brain 129:256–271

Jacquemont S, Hagerman RJ, Hagerman PJ, Leehey MA (2007) Fragile-X syndrome and fragile X-associated tremor/ataxia syndrome: two faces of FMR1. Lancet Neurol 6:45–55

Jensen KB, Dredge BK, Stefani G, Zhong R, Buckanovich RJ et al (2000) Nova-1 regulates neuron-specific alternative splicing and is essential for neuronal viability. Neuron 25:359–371

Jiang H, Mankodi A, Swanson MS, Moxley RT, Thornton CA (2004) Myotonic dystrophy type 1 is associated with nuclear foci of mutant RNA, sequestration of muscleblind proteins and deregulated alternative splicing in neurons. Hum Mol Genet 13:3079–3088

Kashima T, Rao N, Manley JL (2007) An intronic element contributes to splicing repression in spinal muscular atrophy. Proc Natl Acad Sci U S A 104:3426–3431

Kimbell LM, Ohno K, Engel AG, Rotundo RL (2004) C-terminal and heparin-binding domains of collagenic tail subunit are both essential for anchoring acetylcholinesterase at the synapse. J Biol Chem 279:10997–11005

Kimura T, Nakamori M, Lueck JD, Pouliquin P, Aoike F et al (2005) Altered mRNA splicing of the skeletal muscle ryanodine receptor and sarcoplasmic/endoplasmic reticulum Ca2+-ATPase in myotonic dystrophy type 1. Hum Mol Genet 14:2189–2200

Kishore S, Stamm S (2006) The snoRNA HBII-52 regulates alternative splicing of the serotonin receptor 2C. Science 311:230–232

Kondo S, Yamamoto N, Murakami T, Okumura M, Mayeda A et al (2004) Tra2 beta, SF2/ASF and SRp30c modulate the function of an exonic splicing enhancer in exon 10 of tau pre-mRNA. Genes Cells 9:121–130

Koushika SP, Soller M, White K (2000) The neuron-enriched splicing pattern of Drosophila erect wing is dependent on the presence of ELAV protein. Mol Cell Biol 20:1836–1845

Kremer EJ, Pritchard M, Lynch M, Yu S, Holman K et al (1991) Mapping of DNA instability at the fragile X to a trinucleotide repeat sequence p(CCG)n. Science 252:1711–1714

LaFerla FM, Green KN, Oddo S (2007) Intracellular amyloid-beta in Alzheimer's disease. Nat Rev Neurosci 8:499–509

Licatalosi DD, Darnell RB (2006) Splicing regulation in neurologic disease. Neuron 52:93–101

Licatalosi DD, Mele A, Fak JJ, Ule J, Kayikci M et al (2008) HITS-CLIP yields genome-wide insights into brain alternative RNA processing. Nature 456:464–469

Lin X, Miller JW, Mankodi A, Kanadia RN, Yuan Y et al (2006) Failure of MBNL1-dependent post-natal splicing transitions in myotonic dystrophy. Hum Mol Genet 15:2087–2097

Liquori CL, Ricker K, Moseley ML, Jacobsen JF, Kress W et al (2001) Myotonic dystrophy type 2 caused by a CCTG expansion in intron 1 of ZNF9. Science 293:864–867

Manabe T, Katayama T, Sato N, Gomi F, Hitomi J et al (2003) Induced HMGA1a expression causes aberrant splicing of Presenilin-2 pre-mRNA in sporadic Alzheimer's disease. Cell Death Differ 10:698–708

Masuda A, Shen XM, Ito M, Matsuura T, Engel AG et al (2008) hnRNP H enhances skipping of a nonfunctional exon P3A in CHRNA1 and a mutation disrupting its binding causes congenital myasthenic syndrome. Hum Mol Genet 17:4022–4035

Moseley ML, Zu T, Ikeda Y, Gao W, Mosemiller AK et al (2006) Bidirectional expression of CUG and CAG expansion transcripts and intranuclear polyglutamine inclusions in spinocerebellar ataxia type 8. Nat Genet 38:758–769

Mutsuddi M, Rebay I (2005) Molecular genetics of spinocerebellar ataxia type 8 (SCA8). RNA Biol 2:49–52

Ohno K, Milone M, Shen X-M, Engel AG (2003) A frameshifting mutation in *CHRNE* unmasks skipping of the preceding exon. Hum Mol Genet 12:3055–3066

Ohno K, Tsujino A, Shen X-M, Milone M, Engel AG (2005) Spectrum of splicing errors caused by CHRNE mutations affecting introns and intron/exon boundaries. J Med Genet 42:e53

O'Neill JP, Rogan PK, Cariello N, Nicklas JA (1998) Mutations that alter RNA splicing of the human HPRT gene: a review of the spectrum. Mutat Res 411:179–214

Philips AV, Timchenko LT, Cooper TA (1998) Disruption of splicing regulated by a CUG-binding protein in myotonic dystrophy. Science 280:737–741

Query CC, Moore MJ, Sharp PA (1994) Branch nucleophile selection in pre-mRNA splicing: evidence for the bulged duplex model. Genes Dev 8:587–597

Query CC, Strobel SA, Sharp PA (1996) Three recognition events at the branch-site adenine. EMBO J 15:1392–1402

Ranum LP, Cooper TA (2006) RNA-mediated neuromuscular disorders. Annu Rev Neurosci 29:259–277

Rogan PK, Schneider TD (1995) Using information content and base frequencies to distinguish mutations from genetic polymorphisms in splice junction recognition sites. Hum Mutat 6:74–76

Sahashi K, Masuda A, Matsuura T, Shinmi J, Zhang Z et al (2007) In vitro and *in silico* analysis reveals an efficient algorithm to predict the splicing consequences of mutations at the 5′ splice sites. Nucleic Acids Res 35:5995–6003

Sato N, Hori O, Yamaguchi A, Lambert JC, Chartier-Harlin MC et al (1999) A novel presenilin-2 splice variant in human Alzheimer's disease brain tissue. J Neurochem 72:2498–2505

Savkur RS, Philips AV, Cooper TA (2001) Aberrant regulation of insulin receptor alternative splicing is associated with insulin resistance in myotonic dystrophy. Nat Genet 29:40–47

Schwarze U, Starman BJ, Byers PH (1999) Redefinition of exon 7 in the COL1A1 gene of type I collagen by an intron 8 splice-donor-site mutation in a form of osteogenesis imperfecta: influence of intron splice order on outcome of splice-site mutation. Am J Hum Genet 65:336–344

Shapiro MB, Senapathy P (1987) RNA splice junctions of different classes of eukaryotes: sequence statistics and functional implications in gene expression. Nucleic Acids Res 15:7155–7174

Smith PJ, Zhang C, Wang J, Chew SL, Zhang MQ et al (2006) An increased specificity score matrix for the prediction of SF2/ASF-specific exonic splicing enhancers. Hum Mol Genet 15:2490–2508

Soller M, White K (2003) ELAV inhibits 3′-end processing to promote neural splicing of ewg pre-mRNA. Genes Dev 17:2526–2538

Sperling J, Azubel M, Sperling R (2008) Structure and function of the Pre-mRNA splicing machine. Structure 16:1605–1615

Szabo A, Dalmau J, Manley G, Rosenfeld M, Wong E et al (1991) HuD, a paraneoplastic encephalomyelitis antigen, contains RNA-binding domains and is homologous to Elav and Sex-lethal. Cell 67:325–333

Takahara K, Schwarze U, Imamura Y, Hoffman GG, Toriello H et al (2002) Order of intron removal influences multiple splice outcomes, including a two-exon skip, in a COL5A1 acceptor-site mutation that results in abnormal pro-alpha1(V) N-propeptides and Ehlers-Danlos syndrome type I. Am J Hum Genet 71:451–465

Takasugi N, Tomita T, Hayashi I, Tsuruoka M, Niimura M et al (2003) The role of presenilin cofactors in the gamma-secretase complex. Nature 422:438–441

Ule J, Jensen KB, Ruggiu M, Mele A, Ule A et al (2003) CLIP identifies Nova-regulated RNA networks in the brain. Science 302:1212–1215

Ule J, Stefani G, Mele A, Ruggiu M, Wang X et al (2006) An RNA map predicting Nova-dependent splicing regulation. Nature 444:580–586

Wang Z, Rolish ME, Yeo G, Tung V, Mawson M et al (2004) Systematic identification and analysis of exonic splicing silencers. Cell 119:831–845

Wijmenga C, Hewitt JE, Sandkuijl LA, Clark LN, Wright TJ et al (1992) Chromosome 4q DNA rearrangements associated with facioscapulohumeral muscular dystrophy. Nat Genet 2:26–30

Wu S, Romfo CM, Nilsen TW, Green MR (1999) Functional recognition of the 3′ splice site AG by the splicing factor U2AF35. Nature 402:832–835

Young JI, Hong EP, Castle JC, Crespo-Barreto J, Bowman AB et al (2005) Regulation of RNA splicing by the methylation-dependent transcriptional repressor methyl-CpG binding protein 2. Proc Natl Acad Sci U S A 102:17551–17558

Zhang XH, Chasin LA (2004) Computational definition of sequence motifs governing constitutive exon splicing. Genes Dev 18:1241–1250

Zhang XH, Kangsamaksin T, Chao MS, Banerjee JK, Chasin LA (2005) Exon inclusion is dependent on predictable exonic splicing enhancers. Mol Cell Biol 25:7323–7332

Zorio DA, Blumenthal T (1999) Both subunits of U2AF recognize the 3′ splice site in Caenorhabditis elegans. Nature 402:835–838

ARTICLE IN PRESS

JNS-12138; No of Pages 5

Journal of the Neurological Sciences xxx (2012) xxx–xxx

Contents lists available at SciVerse ScienceDirect

Journal of the Neurological Sciences

journal homepage: www.elsevier.com/locate/jns

A novel mutation in SCN4A causes severe myotonia and school-age-onset paralytic episodes

Harumi Yoshinaga [a,*], Shunichi Sakoda [b], Jean-Marc Good [c], Masanori P. Takahashi [c], Tomoya Kubota [c], Eri Arikawa-Hirasawa [d], Tomohiko Nakata [e], Kinji Ohno [e], Tetsuro Kitamura [f], Katsuhiro Kobayashi [a], Yoko Ohtsuka [a]

[a] Department of Child Neurology, Okayama University Graduate School of Medicine, Dentistry, and Pharmaceutical Sciences, Okayama, Japan
[b] Department of Neurology, Kagoshima University Graduate School of Medical and Dental Sciences, Medical School, Kagoshima, Japan
[c] Department of Neurology, Osaka University Graduate School of Medicine, Osaka, Japan
[d] Department of Neurology, Juntendo University School of Medicine, Tokyo, Japan
[e] Division of Neurogenetics, Center for Neurological Diseases and Cancer, Nagoya University Graduate School of Medicine, Aichi, Japan
[f] Department of Pediatrics, Nipponkokan Fukuyama Hospital, Hiroshima, Japan

ARTICLE INFO

Article history:
Received 27 June 2011
Received in revised form 30 November 2011
Accepted 22 December 2011
Available online xxxx

Keywords:
Channelopathy
Na channel
Skeletal muscle
Activation
Slow inactivation
Schwarz–Jampel syndrome
SCN4A

ABSTRACT

Mutations in the pore-forming subunit of the skeletal muscle sodium channel (*SCN4A*) are responsible for hyperkalemic periodic paralysis, paramyotonia congenita and sodium channel myotonia. These disorders are classified based on their cardinal symptoms, myotonia and/or paralysis. We report the case of a Japanese boy with a novel mutation of *SCN4A*, p.I693L, who exhibited severe episodic myotonia from infancy and later onset mild paralytic attack. He started to have apneic episodes with generalized hypertonia at age of 11 months, then developed severe episodic myotonia since 2 years of age. He presented characteristic generalized features which resembled Schwarz–Jampel syndrome. After 7 years old, paralytic episodes occurred several times a year. The compound muscle action potential did not change during short and long exercise tests. Functional analysis of the mutant channel expressed in cultured cell revealed enhancement of the activation and disruption of the slow inactivation, which were consistent with myotonia and paralytic attack. The severe clinical features in his infancy may correspond to myotonia permanence, however, he subsequently experienced paralytic attacks. This case provides an example of the complexity and overlap of the clinical features of sodium channel myotonic disorders.

1. Introduction

To date, over 40 different mutations causing Na channelopathies of the skeletal muscle have been reported in *SCN4A* gene, which encodes for the pore-forming alpha-subunit of skeletal muscle sodium channel [1,2]. The Na channelopathies of the skeletal muscle are clinically classified into hyperkalemic periodic paralysis, paramyotonia congenita, or sodium channel myotonia on the basis of their clinical phenotype. However, phenotypic variability and marked overlap in symptoms have been reported [3–6]. The cases with severe phenotype in the neonatal period highlight the high clinical variability of sodium channelopathies [7,8]. The electrophysiological studies using heterologously expressed channels have shown that the missense mutations produces a gain-of-function defect of the fast gating such as disrupted fast inactivation and enhanced activation, which should result in increased excitability of the muscle membrane. It has been revealed that not only the defect of fast gating but also that of slow inactivation predisposes to paralytic attack, one of the clinical features of Na channelopathies [9,10].

In this report, we present a Japanese boy with skeletal dysplasia who exhibited very severe myotonia in infancy and mild paralytic attack after seven years of age. We identified a novel mutation in the intracellular loop linking segments 4–5 of domain II in *SCN4* and found that the heterologously expressed mutant channel showed enhancement of the activation and disruption of the slow inactivation.

2. Case report

2.1. Clinical features

The patient was delivered naturally and without complications. There is no family history of neuromuscular disease. Seven days after birth, he experienced transient breath-holding episodes with generalized muscle stiffness and facial pallor while crying. At 11 months of age, 30-second-long episodes of apnea arose with

* Corresponding author at: Shikatacho 2-5-1 Department of Child Neurology, Okayama University Graduate School of Medicine, Dentistry, and Pharmaceutical Sciences, Okayama 700–8558 Japan. Tel.: +81 86 235 7372; fax: +81 86 235 7377.
E-mail address: magenta@md.okayama-u.ac.jp (H. Yoshinaga).

0022-510X/$ – see front matter © 2012 Elsevier B.V. All rights reserved.
doi:10.1016/j.jns.2011.12.015

generalized hypertonia; these episodes were so severe that epileptic seizures were once suspected, but ictal EEG recordings did not indicate that this was the case. These episodes spontaneously disappeared, but at the age of two, the patient started to present daily fluctuating myotonia. The patient presented with a mask-like face with blepharospasm, grip myotonia, and dysarthria. These episodic myotonic attacks persisted for several minutes, hours, or even days, with fluctuation and created difficulties in standing, walking and upper-limb mobility. The symptoms seemed to be aggravated by cold (and were relieved during febrile illness) and fatigue, but not by potassium intake or exercise. The CK value fluctuated between 200 and 1000+ and tended to be high during myotonic attacks.

Fig. 1 depicts a generalized inter-episode feature when he was 5 years and 8 months old. Parental consent to present the photograph in Fig. 1 was obtained. He was of Herculean stature and exhibited several characteristic features, such as low-set ears, epicanthic folds, upturned nose, a long philtrum, puckered lips, short neck, hypertropic thighs, atrophic shoulder girdle muscles, pigeon breast, and joint contracture of the elbow. Accordingly, he was initially suspected as having a myogenic type of Schwarz–Jampel syndrome [4,11]. However, immunofluorescence stain for perlecan was normal in biopsied muscle and the histology revealed a nonspecific myopathic change with increased fiber variability. Acetazolamide, mexiletine, and phenytoin had some effect on his myotonic attacks. When these medications were discontinued on the day he underwent generalized anesthesia for the muscle biopsy, he experienced a very severe myotonic attack that involved the respiratory muscle.

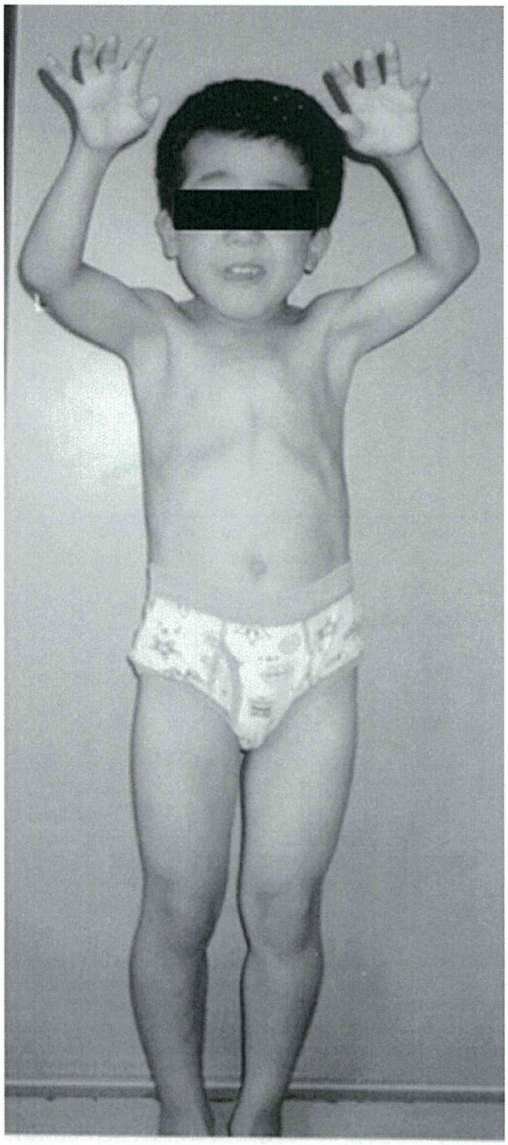

Fig. 1. The patient at 5 years and 8 months of age. Note his Herculean stature and hypertrophic thighs.

After 7 years and 8 months of age, paralytic episodes appeared that occurred several times a year thereafter, even in hot summertime temperatures. He complained of muscle weakness lasting from hours to several days at a time. His mother observed that his thighs become unusually soft during episodes. Neither exercise nor cooling brought about his episodic weakness.

2.2. Clinical electrophysiological analysis

Needle electromyography revealed diffuse continuous myotonic discharges accentuated by needle displacement with dive bomber sounds. Analysis of the compound muscle action potential (CMAP) amplitude before and after short or long exercise revealed no significant change [12]. Muscle cooling did not affect the CMAP either [13].

2.3. DNA analysis

Since there was no expansion of the repeat length at the DM1 locus with Southern blot, we analyzed the nucleotide sequence of *SCN4A* and *CLCN1* genes. Written informed consent was obtained from the parents for the mutation screening. This study was approved by the ethics committee of Kagoshima University Graduate School of Medical and Dental Sciences. Nucleotide sequence analysis of the patient's DNA showed a transition of A to C at the nucleotide in position 2077 (c.2077A>C) in *SCN4A* resulting in the substitution of isoleucine to leucine at amino acid in position 693 (p.I693L) (Fig. 2A). This mutation was not found in the DNA of the parents, both of whom were clinically non-affected. No mutations of *CLCN1* genes were identified by sequencing analysis.

Furthermore, the possibility of Schwarz–Jampel syndrome was excluded by re-sequencing all the exons and the flanking intronic regions of *HSPG2*. We enriched exonic fragments using the SureSelect Human All Exon v2 kit (Agilent, CA, USA), and read 50-bp fragments with the ABI SOLiD 4 sequencer (Applied Biosystems, CA, USA). We mapped 56,007,335 tags (89% of total tags) to human genome GRCh37.3/hg19 with BioScope 1.3.1 (Applied Biosystems), and read 2338 Mbp. Detection of SNVs with Avadis NGS (Strand Life Sciences, Bangalore, India) using default parameters revealed three homozygous missense SNPs that were all registered in dbSNP134 without any reference to clinical relevance (W71S, rs2254357, global minor allelic frequency (GMAF) = 0.475; G242V, rs2254358, GMAF = 0.476; and N765S, rs989994, GMAF = 0.068).

2.4. Sodium channel functional study

We cultured human embryonic kidney (HEK) cells and transfected them with wild-type or mutant human sodium channel constructs as previously described [14]. Na + currents were recorded by the conventional whole-cell patch clamp technique. As shown in Fig. 3A, the mutant channels were consistently activated at more hyperpolarized voltages than the wild-type channels. To further investigate this phenomenon, the normalized sodium conductance at each measured peak current was calculated and plotted against the corresponding voltage. There was a marked shift towards hyperpolarized voltages in the activation curve of p.I693L mutant channels indicating an enhancement of the activation (Fig. 3B. Table 1).

Please cite this article as: Yoshinaga H, et al, A novel mutation in SCN4A causes severe myotonia and school-age-onset paralytic episodes, J Neurol Sci (2012), doi:10.1016/j.jns.2011.12.015

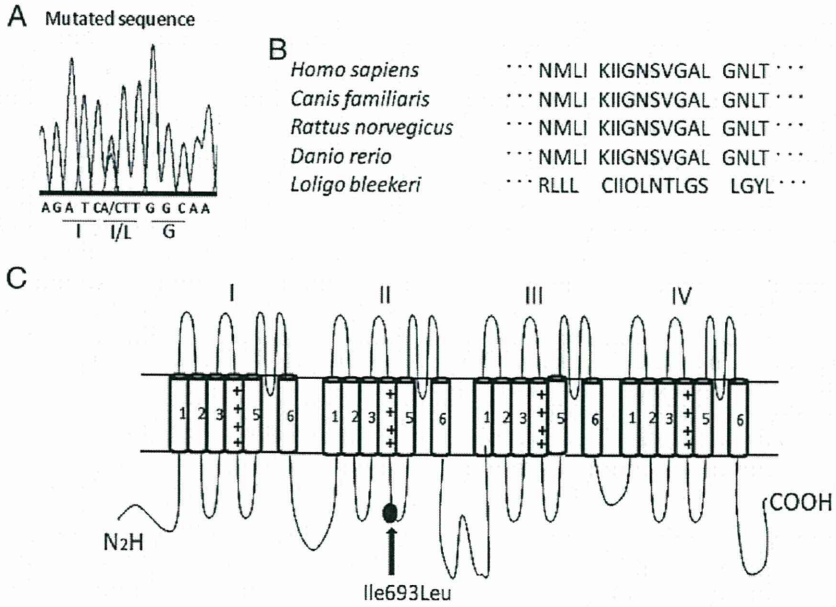

Fig. 2. A: DNA sequencing of the mutant region shows the transition of A to C at the nucleotide in position 2077 resulting in the substitution isoleucine (I) to leucine (L) at aminoacid in position 693 (I693L).B: Isoleucine residue in position 693 in Nav1.4 channel is preserved among homologs in many species.C: Schematic of the α subunit of Nav1.4 channel showing the six transmembrane segments (1–6) of each of the four domains (I–IV) and the location of p.I693L mutation (gray point).

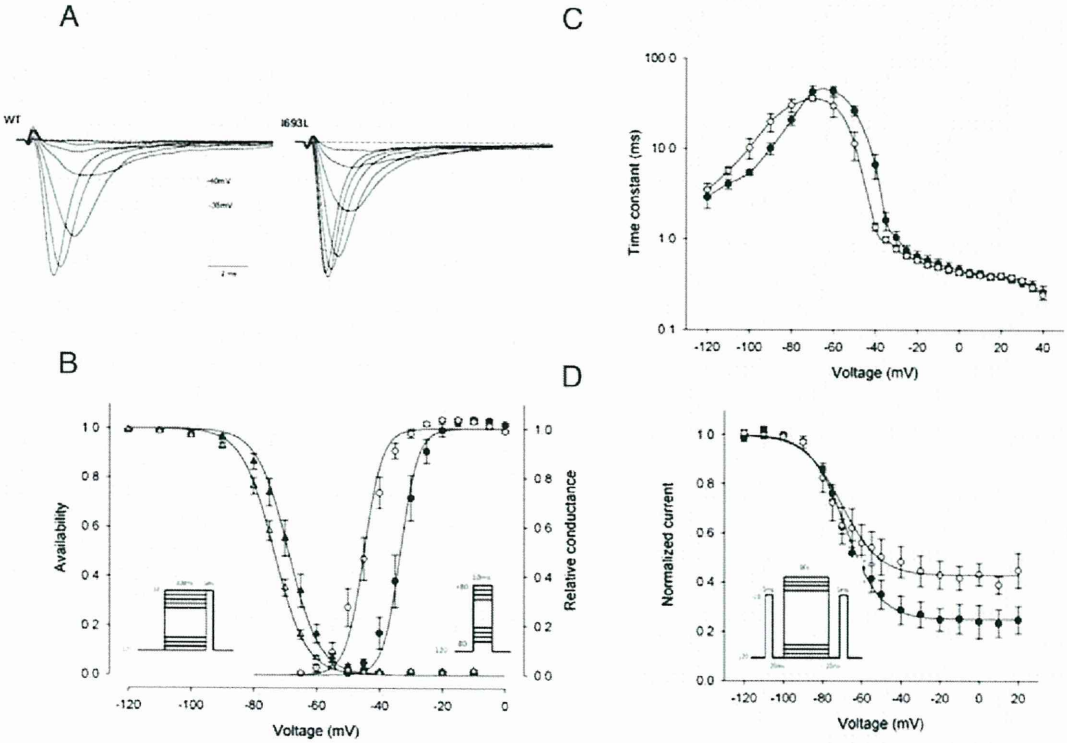

Fig. 3. A: Representative normalized currents recorded from HEK cells transfected with wild-type (WT) and I693L mutant channel and elicited by a series of 10 ms step pulse depolarizations from a holding potential of −120 mV to +40 mV in 5 mV increments. Activation is enhanced in I693L mutant channels.B: Activation (right-hand curves) for the wild-type ○ and I693L ● channels measured as the relative conductance of the peak sodium current elicited by depolarizing pulse from a holding potential of −120 mV to +40 mV (protocol in right inset). The activation voltage dependence of I693L mutant was shifted in the direction of hyperpolarization ($p<0.001$). Steady state fast inactivation (left-hand curves) for the wild-type △ and p.I693L ▲ channels measured as the relative peak current elicited by a −10 mV pulse after a 300 ms conditioning (protocol in left inset). We observed a shift towards negative voltages of the mutant constructs ($p=0.009$).C: Voltage dependence of the fast inactivation kinetics for the wild-type ○ and I693L ● channels measured by combining the data from three protocols (see results): a two-pulse recovery protocol (−120 mV to −80 mV), a two-pulse entry protocol (−70 mV to −40 mV) and a single-pulse relaxation protocol (−35 mV to +40 mV). The time constant for I693L channels was slightly slower at the negative voltages measured with the recovery protocol (n.s. $p>0.05$) and faster at the intermediate voltages measured with the entry protocol (from −50 mV to −35 mV $p<0.05$) than the wild-type. No difference was observed at more depolarized voltage.D: Peak sodium current elicited by a −10 mV test pulse was measured after a 60 s conditioning followed by a 20 ms gap at −120 mV to allow recovery from fast inactivation (protocol in the inset). The maximum extent of slow inactivation (1–I0) was smaller for I693L channels ●, revealing its impairment in comparison with the wild-type ○.

Please cite this article as: Yoshinaga H, et al, A novel mutation in SCN4A causes severe myotonia and school-age-onset paralytic episodes, J Neurol Sci (2012), doi:10.1016/j.jns.2011.12.015

Table 1
Gating parameter for WT and mutant Nav 1.4.

	Activation		Fast inactivation		Slow inactivation		
	V1/2(mV)	*k* (mV)	V1/2(mV)	*k* (mV)	V1/2(mV)	*k* (mV)	I0
WT	−33.3 ± 1.5 (9)	2.8 ± 0.4	−68.9 ± 1.6 (9)	5.0 ± 0.2	−68.3 ± 1.4 (5)	8.9 ± 1.1	0.25 ± 0.0522
p.I693L	−44.9 ± 1.5** (16)	2.9 ± 0.2	−73.5 ± 0.9* (5)	5.1 ± 0.2	−70.1 ± 3.3 (6)	9.6 ± 1.6	0.43 ± 0.0446*

Values are means + S.E.M, with number of experiments in parenthesis * significantly different from WT. P<0.05.
**significantly different from WT. P<0.001.

3. Discussion

Prior to identification of the sodium channel mutation, this patient was initially diagnosed as having a myogenic type of Schwartz–Jampel syndrome because of his characteristic appearance with severe myotonia [1,11]. The confusion between Schwartz–Jampel syndrome and sodium channelopathy was previously reported in a patient with myotonia permanence caused by G1306E mutation of SCN4A [4]. Our patient may also correspond to myotonia permanence, and he exhibited severe myotonic symptoms as apneic episodes from the neonatal period. Several patients with a *SCN4A* mutation, who showed severe symptoms including respiratory distress from an early neonatal period have also been reported [7,8]. One of these cases resembled Schwartz–Jampel syndrome [8].

Our patient showed severe myotonic episodes in his early infancy and then subsequent paralytic episodes. This case provides an example of the complexity and overlap of the clinical features of the sodium channel myotonic disorders, which sometimes make their classification difficult.

Some medications, including local anesthetics, anticonvulsants, and antiarrhythmics such as mexiletine, have shown efficacy for myotonic sodium channelopathies by blocking the sodium channel [2,15]. A carbonic anhydrase inhibitor, acetazolamide, is known to prevent paralytic attack but its antimyotonic action is in question. The myotonia of our patient showed a good response to mexiletine, phenytoin and acetazolamide, although carmabazepin showed little effect. Further studies are needed to understand the difference in efficacy between these drugs and the effects of acetazolamide.

The recently proposed standardized protocols involving short and long exercise tests in electromyographic analysis have improved the diagnosis of the subgroup of mutations in muscle channelopathies [12,13]. Fournier et al. [13] reported that combining the responses to several tests defined five electromyographic patterns that correspond to the subgroups of mutations. We applied their protocol to our patient and defined the response as pattern III [11] in which excitability is not impeded by any of the exercise trials. In their report [11], patients carrying G1306A or I693T (same locus on Nav 1.4 as ours [16]) sodium channel mutation also exhibited pattern III.

Functional analysis of the mutant channel revealed that the activation of the mutant channel was markedly enhanced in concordance with the enhanced excitability of our patient. However hyperpolarized shift of the steady-state inactivation curve which should reduce excitability, was also in a milder way observed in the mutant channel. The former may prevail over the latter, explaining the enhanced excitability which contributes to myotonia. Other mutations such as V445M [17], L689I [18], I704M, including the aforementioned I693T [16], have been found to similarly enhance both activation and fast inactivation and are often associated with myotonia.

Also, our data showed disrupted slow inactivation in the mutant construct, a defect which is expected to predispose to prolonged attack of paralysis. Our patient started to show episodic weakness recently. Again, I693T mutation showed an enhancement of activation with a slight shift towards hyperpolarized voltages for the steady state inactivation as well as a severely impaired slow inactivation [16]. The channel gating defects for I693T and its electromyographic pattern are strikingly similar with those observed for I693L. Unexpectedly, the I693T patient suffered from cold-induced weakness with a very mild myotonia [16]. The difference in hydrophobicity between the two mutated amino acids or the underlining genetic or environmental factors such as drug treatment can possibly modulate the expression of the disease.

Two other mutations, L689I and T70M, have been reported in the intracellular loop linking segments 4–5 of domain II in *SCN4A* [18]. Both have a phenotype of hyperkalemic periodic paralysis with a predominant weakness. The functional analysis of these mutant channels again revealed an enhancement of activation, and an impaired slow inactivation to a similar extent as for I693L mutant. These data and ours confirm the fact that the IIS4-S5 linker is one of the determinant regions for the sodium channel slow inactivation and to a various extent for the activation.

4. Conclusion

Further study of the genotype–phenotype correlations through individual cases will increase our knowledge of the variability of signs in this group of diseases and may also provide us with deeper insight into the function of the various regions of sodium channel proteins.

Acknowledgement

We thank Dr. Steve Cannon, University of Texas, for providing the expression vectors. This study was supported by Grants-in-Aids from the Ministry of Education, Culture, Sports, Science and Technology as well as the Ministry of Health, Labor and Welfare of Japan.

References

[1] Lehmann-Horn F, Rudel R, Jurkat-rott K. Nondystrophic myotonias and periodic paralyses. In: Engel AG, Franzini-Armstrong C, editors. Myology. 3rd ed. New York: McGraw Hill; 2004. p. 1257–300.
[2] Matthews E, Fialho D, Tan SV, Venamce SL, Cannon SC, Sternberg D, et al. The non-dystrophic myotonicas: molecular pathogenesis, diagnosis and treatment. Brain 2010;133:9–12.
[3] Plassart E, Eymard B, Maurs L, Hauw JJ, Lyon-Caen O, Fardeau M. Paramyotonia congenita: genotype to phenotype correlations in two families and report of a new mutation in the sodium channel gene. J Neurol Sci 1996;142:126–33.
[4] Colding-Jorgensen E, Duno M, Vissing J. Autosomal dominant monosymptomatic myotonia premanens. Neurology 2006;67:153–5.
[5] Lerche BH, Heine R, Pika U, George Jr AL, Mitovic N, Browatzki M, et al. Human sodium channel myotonia: slowed channel inactivation due to substitutions for a glycine within the III-IV linker. J Physiol 1993;470:13–22.
[6] Rudel R, Ricker K, Lehmann-Horn F. Genotype–phenotype correlations in human skeletal muscle sodium channel diseases. Arch Neurol 1993;50:1241–8.
[7] Lion-Francois L, Mignot C, Vicart S, Manel V, Sternberg D, Landrieu P, et al. Severe neonatal episodic laryngospasm due to de novo SCN4A mutation. Neurology 2010;75:641–5.
[8] Gay S, Dupuis D, Faovre L, Masurel-Paulet A, Labenne M, Colombani M, et al. Severe neonatal non-dystrophic myotonia secondary to a novel mutation of the voltage-gated sodium channel (SCN4A) gene. Am J Med Genet A 2008;146:380–3.
[9] Goldin AL. Mechanisms of sodium channel inactivation. Curr Opin Neurobiol 2003;13(3):284–90.
[10] Hayward LJ, Sandoval GM, Cannnon SC. Defective slow inactivation of sodium channels contributes to familial periodic paralysis. Neurology 1999;52:1447–53.

Please cite this article as: Yoshinaga H, et al, A novel mutation in SCN4A causes severe myotonia and school-age-onset paralytic episodes, J Neurol Sci (2012), doi:10.1016/j.jns.2011.12.015

[11] Topaloglu BH, Serdaroglu A, Okan M, Gucuyener K, Tope M. Improvement of myotonia with carbamazepine in three cases with the Schwartz–Jampel syndrome. Neuropediatrics 1993;24:232–4.
[12] Fournier E, Arzel M, Sternberg D, Vicart S, Laforet P, Eymard B, et al. Electromyography guides toward subgroups of mutations in muscle channelopathies. Ann Neurol 2004;56:650–61.
[13] Fournier E, Viala K, Gervais H, Sternberg D, Arzel M, Vicart S, et al. Cold extends electromyography distinction between ion channel mutations causing myotonia. Ann Neurol 2006;60:356–65.
[14] Hayward LJ, Brown Jr RH, Cannon SC. Inactivation defects caused by myotonia-associated mutations in the sodium channel III–IV linker. J Gen Physiol 1996;107:559–76.
[15] Heatwole CR, Moxley III RT. The nondystrophic myotonia. Neurotherapeutics 2007;4:238–51.
[16] Plassart-Schiess E, Lhuillier L, George Jr AL, Fontaine B, Tabti N. Functional expression of the Ile693Thr Na+ channel mutation associated with paramyotonia congenital in a human cell line. J Physiol 1998;507(3):721–7.
[17] Takahashi MP, Cannon SC. Enhanced slow inactivation by V 445M: a sodium channel mutation associated with myotonia. Biophys J 1999;76:861–8.
[18] Bendahhou S, Cummins TR, Kula RW, Fu YH, Ptacek LJ. Impairment of slow inactivation as a common mechanism for periodic paralysis in DIIS4-S5. Neurology 2002;58:1266–72.

Please cite this article as: Yoshinaga H, et al, A novel mutation in SCN4A causes severe myotonia and school-age-onset paralytic episodes, J Neurol Sci (2012), doi:10.1016/j.jns.2011.12.015

Perlecan-Deficient Mutation Impairs Corneal Epithelial Structure

Takenori Inomata,[1,2] *Nobuyuki, Ebihara,*[1] *Toshinari Funaki,*[1] *Akira Matsuda,*[1] *Yasuo Watanabe,*[1] *Liang Ning,*[2] *Zhuo Xu,*[2] *Akira Murakami,*[1] *and Eri Arikawa-Hirasawa*[2,3]

Purpose. To elucidate the role of perlecan (Hspg2), a large multidomain heparan sulfate proteoglycan expressed in the basement membrane, in the structure of the corneal epithelium.

Methods. A previously developed perlecan-deficient ($Hspg2^{-/-}$-Tg) mouse model was used. Histologic analysis of their corneas was performed by light and transmission electron microscopy. The localization of perlecan in the corneas of wild-type (WT) mice and $Hspg2^{-/-}$-Tg mice was examined by immunohistochemistry. The effects of perlecan deficiency on corneal epithelial structure was analyzed with respect to the expression of corneal epithelial proliferation and differentiation markers, such as Ki67, cytokeratin12 (K12), connexin43 (Cx43), Notch1, and Pax6 by immunohistochemistry and real-time polymerase chain reaction (PCR).

Results. The $Hspg2^{-/-}$-Tg mice had microphthalmos and a thinner corneal epithelium compared with that of the WT mice. Perlecan was localized in the corneal epithelial basement membrane in the WT mice, but not in the $Hspg2^{-/-}$-Tg mice. The $Hspg2^{-/-}$-Tg corneal epithelium exhibited thinner wing cell layers and a decreased number of Ki67-positive cells, but no dead cells, compared with the WT corneal epithelium. Immunohistochemistry and real-time PCR analysis revealed a significantly decreased expression of corneal epithelial differentiation markers such as K12, Cx43, Notch1, and Pax6 in $Hspg2^{-/-}$-Tg mice, compared with those of the WT mice.

Conclusions. The findings of this study highlight a strong correlation between the presence of perlecan in the basement membrane and the structure of corneal epithelium and that the perlecan-deficient mutation impairs corneal epithelial structure. (*Invest Ophthalmol Vis Sci.* 2012;53:1277–1284) DOI:10.1167/iovs.11-8742

The surface of a mammalian cornea is composed of a nonkeratinized, self-renewing, pluristratified epithelium of ectodermal origin. The corneal epithelium consists of basal, wing, and superficial cells that are separated from the stroma by the basement membrane (BM). Corneal epithelial cells exhibit a dynamic homeostasis, turning over approximately every 7 to 10 days. Many cellular processes, such as proliferation, apoptosis, differentiation, migration, adhesion, and stratification, are essential for the structure of corneal epithelium.

Perlecan (Hspg2) is a large (>400 kDa), multidomain heparan sulfate proteoglycan (Hspg) expressed in BM.[1–6] The protein core consists of five domains that share homology with other molecules involved in nutrient metabolism, cell proliferation, and adhesion, including laminin, the low-density lipoprotein (LDL) receptor, epithelial growth factor (EGF), and the neural cell adhesion molecule (N-CAM).[1–3] Within the protein core there are numerous sites for O-linked glycosylation, as well as four potential sites for heparan sulfate (HS)/chondroitin sulfate (CS) chain attachment. These chains, which are usually HS, have been shown to be involved in many interactions, including those associated with growth factors, extracellular matrix (ECM) molecules, and neuromuscular junction proteins.[1–3,7] Perlecan regulates cells through a basic mechanism involving the binding of various proteins via the protein core and/or the glycosaminoglycan chains. In vertebrates, perlecan functions in a diverse range of developmental and biological processes, from the development of cartilage to the regulation of wound healing.[8–13] Recent reports from other groups also emphasized a key role for perlecan in regulating cell proliferation and cell survival in different tissues. For example, it has been reported that perlecan HS deficiency induces apoptosis of lens epithelial cells.[14] Sher et al.[15] found that perlecan regulates both the survival and terminal differentiation steps of keratinocytes and that it is critical for the formation of normal epidermis.

In the cornea, perlecan is expressed in the BM of the corneal epithelium.[16] However, the functions or roles of perlecan in the cornea have yet to be well investigated. Therefore, in the present study, the role of perlecan in the structure of corneal epithelium was investigated by use of perlecan-deficient ($Hspg2^{-/-}$-Tg) mice. By genetically disrupting perlecan expression in the BM of corneal epithelium, the results of this study revealed that perlecan is essential in the structure of corneal epithelium. To the best of our knowledge, this study is the first to demonstrate the involvement of perlecan in the structure of the corneal epithelium.

Materials and Methods

Animal Experiments

Some perlecan-deficient ($Hspg2^{-/-}$) mice die around embryonic day (E)10 due to defects in the myocardial basement membranes, and the mice that survive this stage die perinatally of premature cartilage development.[12,17] In a previous study, a perlecan transgenic mouse line (Tg, *Col2a1-Hspg2*$^{Tg/-}$) that expresses recombinant perlecan in cartilage was created by use of a cartilage-specific *Col2a1* promoter/enhancer to reverse the cartilage abnormalities of $Hspg2^{-/-}$ mice.[13] Perinatal lethality-rescued mice ($Hspg2^{-/-}$-Tg, $Hspg2^{-/-}$; *Col2a1-*

From the Departments of [1]Ophthalmology and [3]Neurology and the [2]Research Institute for Disease of Old Age, Juntendo University School of Medicine, Tokyo, Japan.

Submitted for publication October 5, 2011; revised November 16, 2011, and January 6, 2012; accepted January 10, 2012.

Disclosure: **T. Inomata**, None; **N. Ebihara** , None; **T. Funaki** , None; **A. Matsuda**, None; **Y. Watanabe**, None; **L. Ning**, None; **Z. Xu**, None; **A. Murakami**, None; **E. Arikawa-Hirasawa**, None

Corresponding author: Nobuyuki Ebihara, Department of Ophthalmology, Juntendo University School of Medicine, 2-1-1 Hongo, Bunkyo-ku, Tokyo 113-8421 Japan; ebihara@juntendo.ac.jp.